Mathematical Statistician and Engineering Applications
ISSN: 2094-0343
2326-9865

Design and Analysis of Effectual Spectrum Sensing Techniques for Aeronautical-Ldacs Using Low-Power Correlators

P. Surendrababu[1], Dr. Vijay Prakash Singh [2]

[1]Research Scholar , Dept. of Electronics and Communication Engineering,Sri Satya Sai University of Technology and Medical Sciences, Sehore Bhopal-Indore Road, Madhya Pradesh, India

[2]Research Guide, Dept. of Electronics and Communication Engineering ,Sri Satya Sai University of Technology and Medical Sciences

Article Info

Page Number: 12501 - 12517

Publication Issue:

Vol 71 No. 4 (2022)

Article History

Article Received: *15 September 2022*

Revised: *25 October 2022*

Accepted: *14 November 2022*

Publication: *21 December 2022*

Abstract

This study's creative, practical equipment synchronizer for L-DACS1 gadgets offers reliable execution at negligible power utilization. Asset use. As per Monte Carlo reproductions, the proposed synchronization procedure gives exact STO assessment notwithstanding fragmentary CFO assessment. Xilinx's xc7z020clg484-1 is a remarkable Field Programmable Door (FPGA) model, proposed using only 6.5%, 3.7%, and 6.4% of the total number of flip-flops, lookup tables, and computerized devices can be used to create a synchronized synchronizer. Signal processing blocks used separately. The unique power of the proposed synchronizer is less than 1mW. Using a Xilinx Zynq FPGA, we tested the proposed scheme and showed that this methodology could save 28.3% power over the multiplier-based approach. Our results further demonstrate that the proposed scheme provides 100% detection accuracy even at -12 dB SNR, rather than energy site-based approaches that often require additional hardware for riot assessmentisshown.

Keywords: *Spectrum Sensing, Low-Power, Correlators, Aeronautical, LDACS*

1. INTRODUCTION

The expansion of computerized handling blocks, which may likewise allow keen and on-request spectrum allotment, can support LDACS's allure in flying frameworks. LDACS proposed the use of mental radio (CR) based proprietary spectrum access. This enables fast, on-demand access to L-Band channels and allows compliance with standard endurance and health requirements. This allows the aircraft to detect open frightening clusters in the air-to-ground spectrum and select the best channel to initiate LDACS air-to-ground transmissions. (1. T. H. Pham, 2014.)Providing dynamic spectrum access for LDACS instead of a terrestrial CR framework presents notable difficulties because the scope of the framework involves constantly moving aircraft. For more effective recognition. Also, to follow weight, space, and power imperatives, answers for airplane should be lightweight and power-proficient; by and by, ground-based frameworks might utilize powerful PCs to meet the handling necessities.

In this article, we propose a spectrum acquisition method using a low-power correlator that also acts as a receiver synchronizer for OFDM basebands. The IEEE 802.16d multiplier-less correlator scheme has been updated to match the LDACS air-to-ground extended prelude design. Besides,

attributable to an assortment of channel conditions, a low transmission power, and the portable idea of the airplane, we improve computational exactness to increment execution in cases with exceptionally low sign to-commotion proportions (SNR). (Fort, 2003)That's what we show, in any event, when the ED procedure consolidates extremely precise commotion forecast, the proposed strategy beats both component location and energy-based traditional spectrum sensing techniques. The multiplier less methodology is the most ideal decision for on-board execution since it emphatically diminishes power utilization. The suggested correlator is developed on a Xilinx Zynq FPGA to test equipment execution.

The rest of this white paper is organized as follows: Part II includes related investigations of spectral sensors, correlator, and FPGA-based mental radio scaffolds. A portrayal of the information outline design and the LDACS standard, which are both used in air-to-ground correspondences, is given to a limited extent III. (K.-W. Yip, , 2003.)To some degree IV, the engineering of the proposed multiplier-less correlator for the LDACS outline is given, alongside a clarification of how it functions with our radio stage. Under various sign quality circumstances, we assess the proposed design in Segment V and contrast it with the ED and FD procedures for LDACS.

2. REVIEW OF LITREATURE

2.1 Spectrum Sensing

The objective of CR-based correspondence frameworks is to utilize unutilized segments of authorized spectrum by giving approaches to progressively get to these spectrum holes. Because of CR's capacity to allow gadgets to entrepreneurially time-share spectrum, there is an expansion in how much accessible transmission capacity and ghostly effectiveness. For CR frameworks, productive ghostly entire discovery is a fundamental condition. In the writing, various systems for finding spectrum openings are examined, each with an unmistakable measure of viability (regarding the chance of tracking down a phony problem) and computational intricacy. (G. Eichinger, 2012) Both straightforward strategies, like energy identification (ED) H. Urkowitz 1967, and computationally serious techniques, like matching channel location, are incorporated. ID of cyclostationary highlights by J. G. Proakis in 2001 Utilizing Eigen esteem discovery with T. Yucek 2009 among others, Y. Zeng 2009. ED has frequently been the most popular and generally utilized approach because of its confused nature and modest PC intricacy. By the by, the precision of ED-based spectrum sensing is essentially affected by the nature of the commotion change assessment. The SNR limit for effective identification is lower with ED-based methods, yet they additionally battle to recognize authentic and fake clients. (K. Le, 2013)Utilizing an energy-contrast based discovery approach for LDACS correspondence, the creators of L. K. Mathew 2016 upgrade customary ED; regardless, assessing mistakes in noise is as yet inclined.

Eigen esteem discovery decides whether correspondence is available or missing in the ongoing station by contrasting the biggest with lowest proportion of the Eigen upsides of the covariance network of the got signal with an edge. Another incomprehensible location strategy, Y. Zeng 2009. However, the formation of a covariance lattice and the decay of the approaching sign into its Eigen values give computationally requesting errands in Eigen esteem identification. The difficult issue of

limit setting for Eigen esteem identification further confines the utilization of this innovation in low power gadgets.

Between commotion (or unlawful client transmissions) and allowed client correspondence, reasonable discovery methods might have the option to differentiate. Cyclostationary include T. Yucek 2009 and matching channel identification are two models. To confirm whether correspondence is happening on a specific channel, cyclostationary include recognition dissects the cyclostationary properties of gotten signals. Nonetheless, the methodology calls for a ton of time spent observing to achieve high discovery exactness, and breakdown of the cyclostationary properties likewise requires a ton of computational work. (K. Amiri, 2007) The edge structure, pilot image design, and testing recurrence of the communicated signal must likewise be known for matched-channels to give the ideal location. Matching channel sensing requests a ton of PC exertion, much as cyclostationary highlight acknowledgment, since the information signals should initially be demodulated before the matched separating method can be applied.

2.2 Multiplier less Correlator in OFDM Systems

OFDM is a regulated technique used in high-throughput remote organizations, offering spectral distribution adaptability and resilience to multipath blurring. OFDM turns into a vital plan in CR frameworks on the grounds that to its help for strategies like spectrum pooling, which allows unlicensed clients impermanent admittance to authorized (inactive) spectrum, and as an outcome, normally empowers dynamic spectrum access. Recio, A. 2010 Compelling OFDM frameworks have a huge test with recipient synchronization since even little mistakes might bring about obstruction between transporters or images. Hanzo, L. 2006.

Numerous methods for accomplishing precise synchronization have been proposed in the writing. They either rely upon techniques in light of cross-relationship which give more noteworthy execution at low SNR rates with exceptionally modern execution, or on autocorrelation-based approaches C. Nanda Kishore 2006 T. M. Schmid 1997), or they consolidate the two as flowed stages, which give a low intricacy execution yet execution that endures incredibly at low sign strength (low SNR). The current year's T.- H. Kim model joins the best of the two universes. (. Lotze, 2009) Anyway there have been ideas for successful cross-correlator executions. They are still almost multiple times more confounded than powerful executions of regular autocorrelations starting around 2003. The referred to preface should be communicated as an amount of powers of 2 to settle this issue utilizing a multiplier less correlator and shift-add blocks rather than duplication. It has been shown that they utilize significantly less assets while keeping up with a similar level of synchronization accuracy as a multiplier-based correlator.

3. LDACS AIR-TO-GROUND COMMUNICATION

An organization of elevated and ground stations called LDACS uses cell innovation to impart (AS).

As recently referenced, LDACS utilizes the OFDM tweak conspire, which has a FFT length of 64 and a joined data transfer capacity of 0.5 MHz for each channel. It utilizes 50 sub-transporters that are 9.8 KHz separated to move information. (S. Shreejith, 2015) For use in aerial and ground-to-

ground correspondence, they are additionally isolated into two banks, each with 25 subcarriers. As per LDACS, these connections are alluded to as the Forward Connection (FL) and Turn around Connection (RL), individually.

In the RL piece of this exploration, we analyze the case for airplane entrepreneurial spectrum access. This makes it workable for airplane to recognize RL band spectrum use, pinpoint the ideal portion, and solicitation authorization from the beginning to utilize that spectrum. (B. Ronak and S. A. Fahmy, 2017.) The ground station might acknowledge the utilization of a proposed channel in light of its overall information on spectrum use in the event that there are no likely struggles. This type of unique spectrum access allows more effective use of the limited RL spectrum, especially in congested airspace.

RL transmission in LDACS depends on OFDM-TDMA blasts that might adjust to the necessities of various clients. While the transmitter configuration is similar to that of a regular OFDM transmitter, versatile coding and regulation strategies are upheld to deal with conditions when there is a ton of obstruction, support high-need messages, and keep up with gathering quality. The Backwards Quick Fourier Change (IFFT) process partitions the adjusted information across a few sub-transporters.

The beneficiary block is equivalent to an ordinary OFDM collector yet contains upgrades to decrease impedance from neighbouring distance estimation hardware (DME) channels (blanking nonlinearity block). Prior to separating the approaching information, the Quick Fourier Change (FFT) block demodulates the sign and afterward performs evening out, demodulation, and deciphering. In a multi-outline, synchronization rationale sets the starting point.

The hierarchy of correspondence in RL is shown in Figure 1. Communication is coordinated by periodic instances of super housing, each lasting 240 ms.

The airplane looks for cell section utilizing four multi-edges and one irregular access opening for each super casing. Each diverse comprises of an information section and a Committed Control (DC) portion of configurable size. Our goal is to progressively empower the multi-outline segment, which is presently physically dispensed to various airplanes by the suitable ground station.

Figure 2 shows the mind boggling outline plan of a RL DC segment with four tiles. The organization's tiles are organized into 6 lines (the arrangement's time space) and 25 sections, with each tile addressing 720 seconds (recurrence space). Likewise, each line has a cyclic prefix (CP), which denotes the beginning of each column in the time-space (not displayed in Fig. 1). (Ambede, 2016) The primary tile, alluded to as the synchronization tile, helps the ground station in synchronizing the LDACS get chain by including the AGC preface, two synchronization images, two pilot images, and a rehash of the AGC prelude. The synchronization tile is a requirement for each RL section, subsequently searching for it at standard stretches may tell whether the portion is being utilized at the present time. The excess tiles are comprised of information handed-off to the ground segment, with pilot images mixed haphazardly.

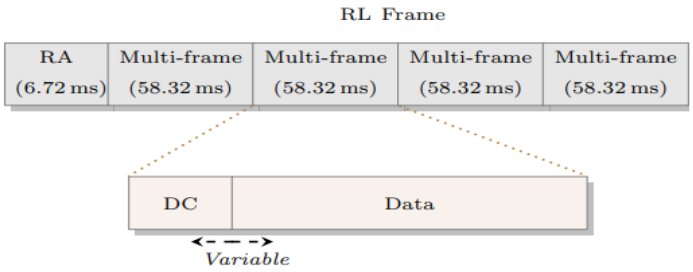

Figure 1: The communication's framing structure for LDACS RL

The FL edge's synchronization tile is correspondingly rested up, but it simply involves the synchronization images rather than an entire tile. To identify when an edge begins and change the example timing window to lessen between image impedance at the airplane collector, the airplane must have the option to perceive the synchronization signal while it is getting a casing starting from the earliest stage. (R. F. A. Tani and D. Marabissi, 2016.)A similar synchronizer block found in the plane collector might be used to precisely get flags and distinguish correspondence in the RL DC segment when the airplane wishes to communicate (when the airplane gets information starting from the earliest stage). Since transmission and gathering happen at independent times, this is doable.

4. LDACS1 SYNCHRONIZATION

The two parts of OFDM synchronization are STO assessment and CFO assessment. STO gauge searches for the main example of each OFDM signal to get a total OFDM image for demodulation. CFO gauge is utilized to decide the recurrence error between tests conveyed and got at the transmitter and beneficiary. (T. L.-N. M. Derakhshani and M. Nasiri-Kenari, , 2011.) The beneficiary might do synchronization utilizing the particular images known as introduction that are sent toward the start of each actual edge. To assign L-DACS1, there are two prelude images required. The time space waveform of the principal image comprises of four indistinguishable areas of length L, while the subsequent image comprises of two indistinguishable bits of length 2L. The L-DACS1 standard characterizes L = 16 Nov as the oversampling factor for beneficiary Nov. Usually 4. The prelude of L-DACS1 is shown in the time domain in Figure 1 after windowing and cyclic prefix (Tcp) addition (Tw).

As characters are transmitted through a particular recursive channel, they are distorted by a zero-mean complex white Gaussian tone. At the receiver, the characters are intercepted and converted to baseband for demodulation. A summary of the example drawing obtained is as follows:

$$r_n = e^{j(2\pi\epsilon n/N)} \sum_{l=0}^{c-1} h_l x_{n-l} + \eta_n \quad (1)$$

Where xn and rn, separately, represent communicated and got tests. Shows the distinction in transporter recurrence between the transmitter and beneficiary in standardized structure. hl is what might be compared to the discrete-time channel drive reaction of length C.

4.1 Proposed Timing Metrics

We propose a new timing estimation method using the connection and preamble structure of L-Energy DACS1. Considering the random component of the main opening image, we make two autocorrelation estimates:

$$\mathbf{AC1}(\boldsymbol{n}) = \sum_{\boldsymbol{m=0}}^{\boldsymbol{2L-1}} \boldsymbol{c1}(\boldsymbol{m},\boldsymbol{n})$$

$$\mathbf{AC2}(\boldsymbol{n}) = \sum_{\boldsymbol{m=0}}^{\boldsymbol{2L-1}} \boldsymbol{c2}(\boldsymbol{m},\boldsymbol{n})$$

$$\boldsymbol{C1}(\boldsymbol{m},\boldsymbol{n}) = \boldsymbol{r}^{*}_{\boldsymbol{n-m}}\boldsymbol{r}_{\boldsymbol{n-m-L}}$$

$$\boldsymbol{c2}(\boldsymbol{m},\boldsymbol{n}) = \boldsymbol{r}^{*}_{\boldsymbol{n-m}}\boldsymbol{r}_{\boldsymbol{n-m-2L}} \quad \textbf{(2)}$$

Where means the intricate formation. The main introduction image is looked for utilizing the principal autocorrelation measure, which finds a quarter rehash, and a half redundancy utilizing the subsequent autocorrelation measure. Both edge ID and a precise CFO gauge, which are introduced To some degree II-B, are finished utilizing these techniques.

The got image energy is estimated utilizing a proposed energy meter named ENE during the length of a 2-L period. This number goes about as a measuring stick for recognizing a looming preface.

$$\mathbf{ENE}(\boldsymbol{n}) = \textstyle\sum_{\boldsymbol{m=0}}^{\boldsymbol{2L-1}} \boldsymbol{r}^{*}_{\boldsymbol{n-m}} * \boldsymbol{r}_{\boldsymbol{n-m}} \textbf{(3)}$$

To keep the clarification straightforward, expect an ideal channel with clam or. Then, utilizing the models below, proclaim the got preface:

$$\boldsymbol{r_n} = \boldsymbol{e^{j}}(\boldsymbol{2\pi} \in \boldsymbol{n/N}) * \boldsymbol{p_n} + \boldsymbol{n_n} \quad \textbf{(4)}$$

The preamble symbol transmission samples are denoted by the letter pn. The metrics in (2) are obtained as follows:

$$\mathbf{AC1}(\boldsymbol{n}) = \boldsymbol{e}^{-j\emptyset_1} \sum_{\boldsymbol{m=0}}^{\boldsymbol{2L-1}} \boldsymbol{P}^{\boldsymbol{2}}_{\boldsymbol{n-m}} + \eta\mathbf{1}(\boldsymbol{n})$$

$$\eta\mathbf{1}(\boldsymbol{n}) = \textstyle\sum_{\boldsymbol{m=0}}^{\boldsymbol{2L-1}} \eta^{*}_{\boldsymbol{n-m}}\, \eta_{\boldsymbol{n-m-L}} + \boldsymbol{p}_{\boldsymbol{n-m}}(\eta^{*}_{\boldsymbol{n-m}} + \eta_{\boldsymbol{n-m-L}}) \quad \textbf{(5)}$$

Where 1(n) is the noise element of the metric. CFO causes a phase rotation with the formula 1 = 2(L/N). The outcomes for ENE (n) and AC2(n) are comparable:

$$\mathbf{AC2}(\boldsymbol{n}) = \boldsymbol{e}^{-j\emptyset_2} \sum_{\boldsymbol{m=0}}^{\boldsymbol{2L-1}} \boldsymbol{p}^{\boldsymbol{2}}_{\boldsymbol{n-m}} + \eta\mathbf{2}(\boldsymbol{n})$$

$$\mathbf{ENE}(\boldsymbol{n}) = \sum_{\boldsymbol{m=0}}^{\boldsymbol{2L-1}} \boldsymbol{P}_{\boldsymbol{n-m}}^{\boldsymbol{2}} + \eta_{\boldsymbol{e}} \qquad \textbf{(6)}$$

Where the stage pivot part and commotion part of the second autocorrelation metric, separately, are 2(n) and 2 = 2(2L/N). E represents the energy metric's clam or part. At the point when the main preface image is gotten, the autocorrelation measurements equivalents the energy metric on the off chance that the clam or piece and stage turn part are negligible.

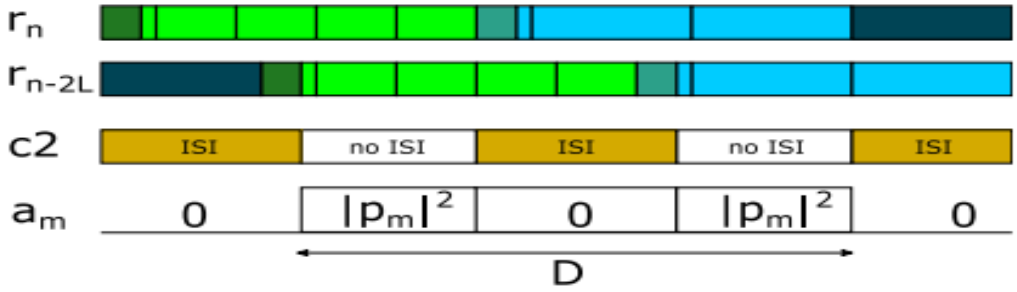

Figure 2: Suggested Metrics for Correlating with the L-DACS1 Prologue.

T samples	Amplitude
21	1.2
28	2.5
32	3.6
39	3.8
42	4.2
50	5.1

Table 1:STO estimation metrics using cross-correlation at SNR = 10 dB.

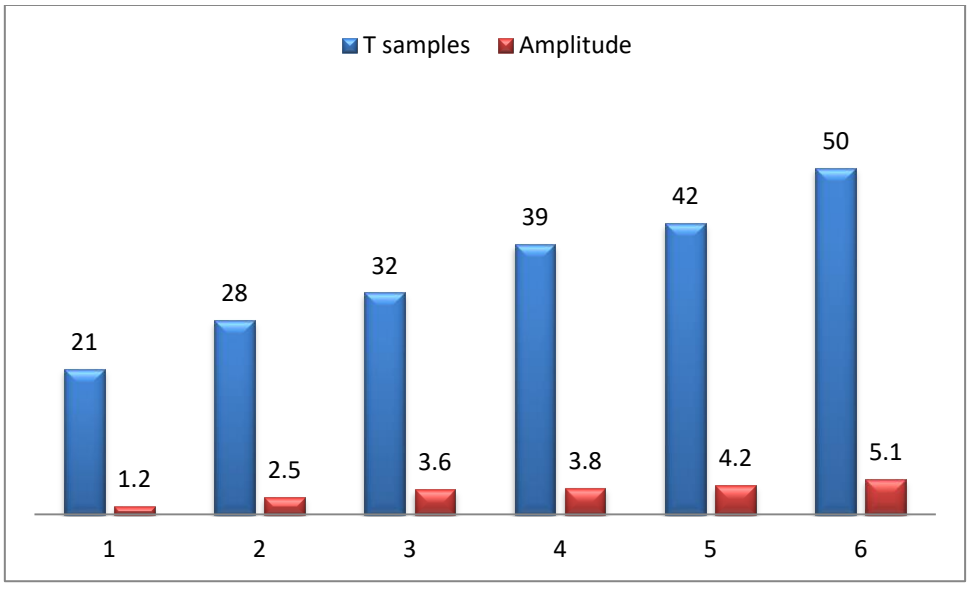

Figure 3: STO estimation metrics using cross-correlation at SNR = 10 dB.

An energy relationship measure is introduced as an option in contrast to the more traditional system of involving signal cross connection for an effective STO gauge. There is no association with the

energy. Am is a transmission prelude energy vector, and the proposed measurement substitutes prompt energy r n m rn m for immediate energy r n m rn m. The vector am shown in Fig. 2 has a length of D. At the point when preface images are remembered for the got signal, it is critical to take note of that |c2(m, n)| approaches the moment energy. Coincidentally, considering the way that ISI happens when they got signal copies with its deferred structure, |c2(m, n)| kills a periodic piece of the preface as tracked down in Fig. 2. (V. K. S. Chaudhari and H. V. Poor, 2009)Subsequently, the recommended measure can diminish optional pinnacles, expanding STO gauge exactness.

Figure portrays the standardized qualities (XCR) of the recommended measurement. 3 notwithstanding moment energy connection (XEne) and signal cross relationship (XSig). The right STO where the biggest pinnacle seems is = 0 as should be visible.

In contrast with XSig and XEne, the recommended metric's auxiliary tops at 64 and 64 (i.e., L and L) are more modest.

5. SIMULATION

For L-DACS1 frameworks, Monte Carlo reenactments are utilized to survey the recommended strategy. In MATLAB, we analyze how well synchronization performs for both AWGN and aeronautical spread channels. For every model, 10,000 preliminaries are reproduced. For STO and CFO computations, individually, the bomb rate and mean square mistake (MSE) are utilized to measure how exact the synchronization approach is. The disappointment rate is the extent of inaccurate timing expectations made from all preliminaries (i.e., 10 000 times). In light of the error between CFO assessment and genuine CFO, not entirely settled.

5.1 Performance in AWGN Channels

In AWGN channel with the presence of CFO, the presentation of the proposed strategy is analyzed as opposed to the SOA technique gave in. The differentiation is displayed as far as the accuracy of fragmentary CFO gauge and time synchronization. The exactness of CFO assessment is evaluated regarding MSE, though STO execution is checked as far as disappointment rate (%).

The viability of time synchronization in AWGN diverts is found in Fig. 4. The recommended arrangements under the situations of a major CFO and a CFO nonattendance are meant as endlessly prop 1.5, individually.

To rise to 1.5 subcarrier separating, the huge CFO is set. SOA and SOA represent the exhibition of the customary methodology in. Utilizing the accuracy of a coarse STO assessment, SOA is surveyed. This demonstrates that assuming STO gauge is in cyclic prefix length, it is accomplished to time synchronization.

By and by, L-DACS1 requests a STO gauge exactness of under 1/11 cyclic prefix length . For fine STO gauge, which requests an exactness of under 1/11 cyclic prefix length, SoA', Endlessly prop 1.5 are estimated. As displayed in Fig. 4, the recommended procedure is impervious to a sizable CFO. Endlessly prop 1.5 both come up short at an almost equivalent rate. The recommended approach effectively assesses the STO within the sight of significant CFO at SNRs more prominent

than 5 dB. With a measure of STO gauge exactness more modest than 1/11 cyclic prefix length, the recommended strategy beats the SoA'. For low SNRs — under 3 dB — the recommended strategy beats the SoA as far as bomb rate. The SoA does coarse STO assessment, though the proposed approach truly does fine STO assessment. Thus, when SNR is higher, SoA exactness rises a tad faster than that of the recommended procedure. Thus, there is a hybrid at 4 dB SNR. The two methodologies offer high precision at SNRs more prominent than 6 dB. After the SoA technique, an exact STO gauge is likewise essential. This approach requires additional computation and takes most of a day to evaluate up to 0.25 seconds at high SNRs. The proposed approach can achieve a fine STO in the preamble 240s time span.

MSE of Fractional CFO	SNR (dB)
10	1.3
15	2.2
19	2.5
22	3.6
2	3.9
31	4.2
36	5.2

Table 2: Efficacy in the Aerospace Communication Sector

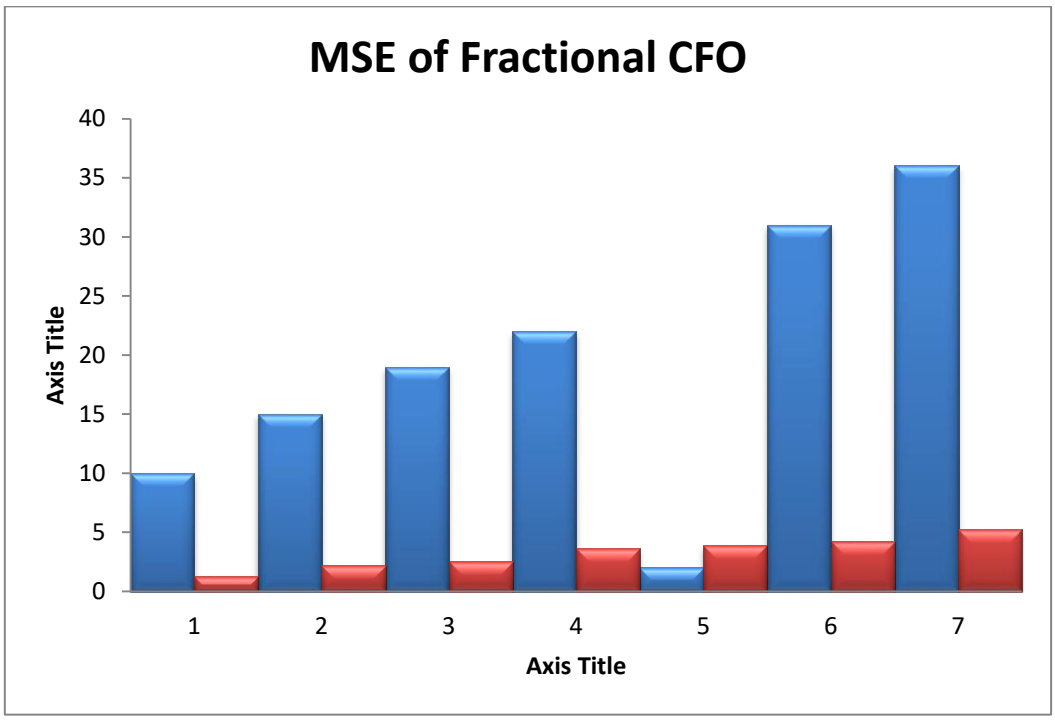

Figure 5: Execution of recurrence offset assessment in AWGN channels

The accuracy of the CFO measurement with AWGN redirection can be seen in Figure 5. SoA and SoA 1.1 separately present the accuracy of the CFO measurement of the SoA methodology in terms of CFO and large CFO. It is resolved that the huge CFO approaches 1.1 subcarrier dividing. The precision of the evaluations utilizing the AC1 and AC2 measures, individually, is shown by AC1

and AC2. On the primary image of the introduction, these assessments are made. Endlessly prop 1.5 show, separately, the assessment exactness of the recommended strategy within the sight of CFO nonattendance and large CFO.

To rise to 1.5 subcarrier separating, the large CFO is set. As displayed in Figure 5, the CFO assessment utilizing the AC2 measure is more exact than the AC1 metric. The presentation of the recommended approach and the SOA technique is practically the same. Prop and SOA are more precise than AC2 since these strategies are completed on two preface images as opposed to the primary prelude image. Besides, SOA 1.1 proposes that in cases with enormous CFO, the SOA strategy's precision endures essentially. Prop is equivalent to Prop 1.5. This shows that the proposed approach keeps on working great in any event, when the CFO is set to 1.5 subcarrier dispersing

5.2 Efficacy in the Aerospace Communication Sector

The recommended synchronization approach in aeronautics directs is analyzed in more detail in this segment. (A. Langowski, 2007)The diverts are displayed in certifiable circumstances such on the way (ENR) trips without/with DME impedance and terminal moving (TMA) regions. The channel model's reproduction boundaries are taken from [13] and [18]. The channel models accommodate an assortment of remote channel peculiarities, including as channel impedance, stage commotion, Doppler spread, and defer spread. Solid view and reflected pathways with postponements of 1 = 0.3 s and 2 = 15 s were utilized to address the ENR channel.

A 1360 km/h most extreme plane speed is thought of, meaning a greatest Doppler shift of 1250 Hz. Utilizing a greatest course postponement of 10 s, a Rican element of 10 dB, and a most extreme Doppler shift of 624 Hz, the TMA channel was re-enacted. For the district encompassing Paris, which has the biggest convergence of DME ground stations in Europe, a reasonable model gave in used to re-enact DME impedance. There are three DME impedance sources in this DME obstruction model, each with a heartbeat pace of 3600 heartbeat matches each second. The principal DME channel is situated at a 0.5 MHz offset from the essential L-DACS1 recurrence. 67.9 DBM of obstruction from this channel is available at the L-DACS1 Rx input. The impedance levels on the other two channels, which are counterbalanced by +0.5 MHz are 74 and 90.3 DBM

Fail rate of time synchronisation	**SNR (dB)**
16	1.2
18	2.3
22	2.5
26	3.6
31	4.9
36	5.2
41	6.1

Table: 3 Time synchronization performance in aeronautical channels

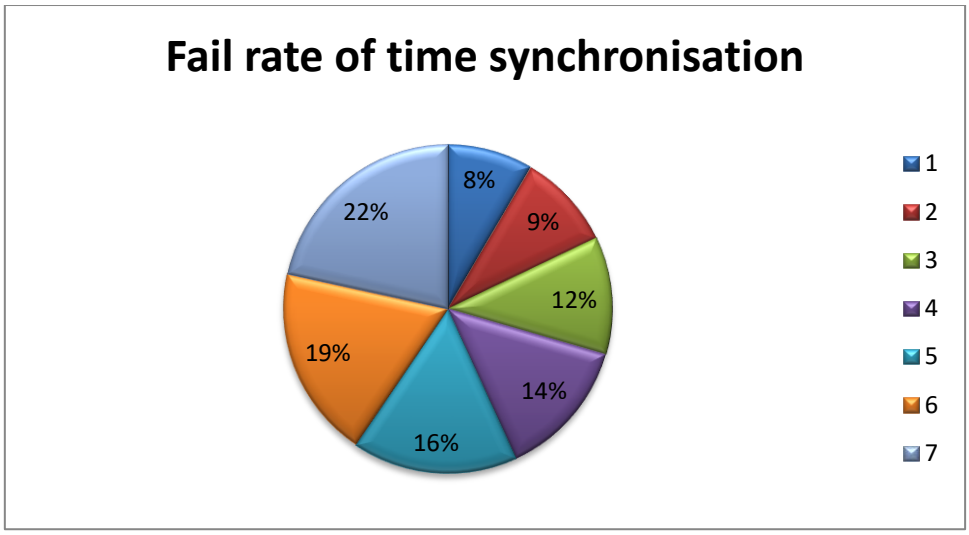

Figure 6: The precision of time-keeping in aviation channels

The proposed strategy's worldly synchronization and CFO gauge execution in the previously mentioned circumstances of flight diverts is displayed in Figs. 6 and 7, separately, alongside a correlation with its exhibition in AWGN channels. ENR-DME recommends what happens in ENR channels with DME impedance, while ENR addresses synchronous execution in ENR channels without DME impairments. TMA stands for synchronous representation in TMA context. As shown. As shown in Figures 6 and 7, when the ENR channel is used without DME impedance, the STO and CFO estimation accuracy is somewhat less accurate than when the AWGN channel is used.

With SNRs higher than 8 dB, the recommended approach can create extraordinary precision in the ENR channels. Tragically, the exhibition of the recommended method endures altogether when DME obstruction is available in ENR channels. STO and CFO gauge exactness are decreased by around 10 and 4 dB, individually. Just at SNRs surpassing 20 dB is the time synchronization prepared to do superior execution. At the point when synchronization happens by means of a TMA channel instead of an AWGN or ENR channel, the presentation is basically same. While STO gauge of TMA essentially improves with SNRs more than 10 dB and accomplishes a decent precision at SNRs over 22 dB, CFO exactness of TMA immerses at SNRs over 10 dB.

MSE of Fractional CFO	**SNR (dB)**
13	2.3
18	2.8
21	3.9
26	4.5
31	4.9
39	5.2
41	6.6

Table 4: Frequency offset estimation performance in aeronautical channels.

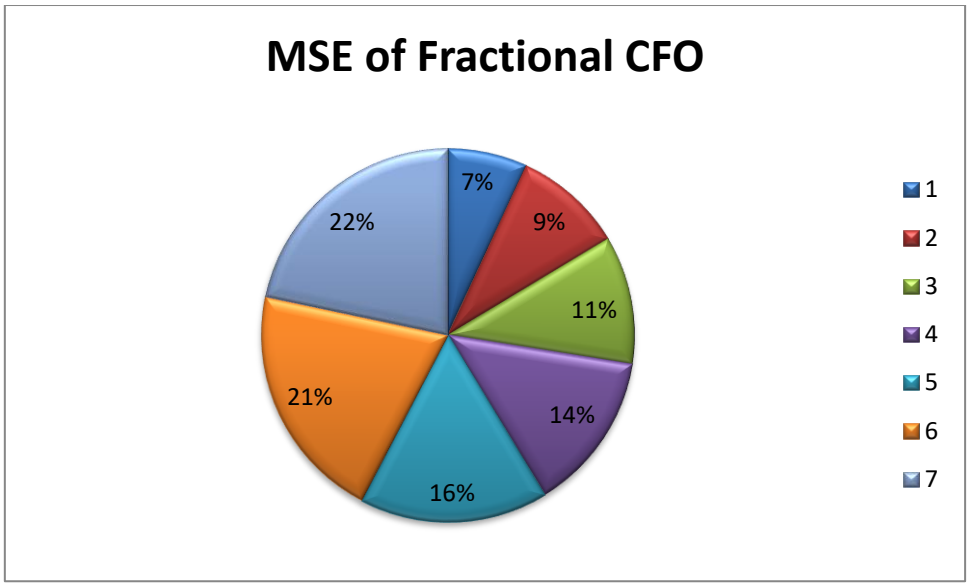

Figure 7: Aviation channel frequency offset estimate performance**.**

6. HARDWARE IMPLEMENTATION

This part looks at the execution of the recommended arrangement, which depends on word size exactness and multiplier less procedures, as well as the equipment utilization enhancement.

The objective FPGA is a Xilinx Zynq-7000 xc7z020clg484-1 gadget, which is found on the Zed board improvement board. Equipment asset and power utilization are evaluated utilizing Vivado 2016.1. The results feature the compromise between the proposed strategy's exactness and equipment use.

The real equipment design used to do the proposed synchronization approach depicted To some degree II is first displayed in the execution. From that point forward, the painstakingly analyzed lowered accuracy of measurements values is utilized to decide the tradeoffs between further developing equipment use proficiency and lowering precision. To some degree IV-C, an extraordinary productive hardware for multiplier less relationship is recommended to additionally diminish how much equipment required. Finally, the execution results were introduced along with an examination of the computational modules in the proposed synchronizer and elective plan enhancements.

6.1 Implementation of Proposed Synchronizer

Fig. 8 portrays the engineering of our recommended method.

The following formulae are utilized in execution to modify the autocorrelation measurements in (2) and (3) to such an extent that they might be registered in a recursive style:

$$\boldsymbol{AC1(n) = AC1(n-1) + c1(0,n) - c1(2L, n-2L)}$$

$$\boldsymbol{AC2(n) = AC2(n-1) + c2(0,n) - c2(2L, n-2L)}$$

$$\boldsymbol{ENE(n) = ENE(n-1) + ee(n) - ee(n-2L)} \quad \textbf{(7)}$$

In which ee(n) = r n r n. These measurements are processed utilizing three-input adders, as displayed in Fig. 8. For the related measurements calculation, the most recent 2L upsides of c1, c2, and ene are supported utilizing the Postpone 2L blocks. The past worth of the measurements is put away in registers. The operands c1 and c2 are registered utilizing a typical getting cushion that contains two blocks of postpone L. The upsides of AC1, AC2, and c2 for CFO and STO gauges are changed over from rectangular to polar structure utilizing three stage interpretation blocks.

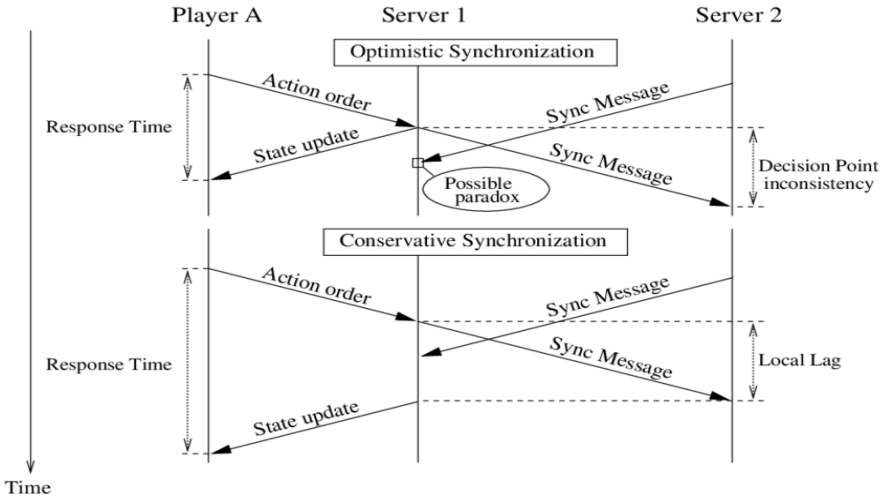

Figure 8: Design of the infrastructure needed to use the suggested synchronization technique

To work the Stage Interpretation blocks, we utilize the Xilinx CORDIC IP centre. In view of multiplierless relationship, the Energy Cor. blocks figure the XCR metric as per condition (6).

Segment IV-C presents a better multiplier less relationship design that is recommended for this block. The Fre. Counterbalance Assessment block utilizes the points of the AC1 and AC2 measurements, which it gets from the Stage Interpretation blocks, to appraise the CFO as per (10) in view of those measurements. Once the rule analyzed by the Comparator block is satisfied, the Timing Sync block looks for peaks in the XCR metric and scores the STO as shown in (7).

6.2 Implications of Less Accuracy

In this part, we consider word length improvements. The effect of reducing the word length is taken into account to protect the accuracy of the evaluation. Assumedly, the got tests are addressed in twos supplement fixed point Q1.15 design and have gone through standardization. This demonstrates that the upsides of the example's genuine and nonexistent parts are under 1, and each part's qualities are addressed by a sum of 16 pieces, including a sign piece and 15 fragmentary pieces.

Let f1, f2, and fe be the set of patches that encode the subparts that process c1, c2, and ee separately. The positive side of the moment autocorrelations c1 and c2 and the moment energies ee

are scaled to be less than one. As a result, c1, c2, and ee have the individual types of Q1.f1, Q1.f2, and Q1.fe. As the autocorrelation measurements are determined on a summation of 2L examples, or 128 examples, the upsides of the measurements are more modest than 128 and just 8 pieces are expected for portrayal in twos supplement to forestall summation overflow.

As a result, Q8.f1, Q8.f2, and Q8.fe, respectively, indicate the AC1, AC2, and ENE measurements.

Besides, we expected that the extent of c2 (i.e., |c2|) was of the structure Q2.fx. To forestall overflow welcomed on by the interpretation of the mind boggling number c2, how much number pieces in |c2| is set to rise to 2. To use the multiplier less relation, standardize the vector am in condition (6) and quantize it to 0.5. The vector am contains 132 nonzero coefficients represented in the L-DAC1 preamble. Along these lines, the upsides of XCR are less than 256 and just a 8-cycle positive number is expected to address them to forestall overflow. Accordingly, Q8.fx shows the XCR metric.

The autocorrelation measurements decide the CFO gauge's rightness, and the examination of the autocorrelation measurements and the ENE metric is important for the STO assessment.

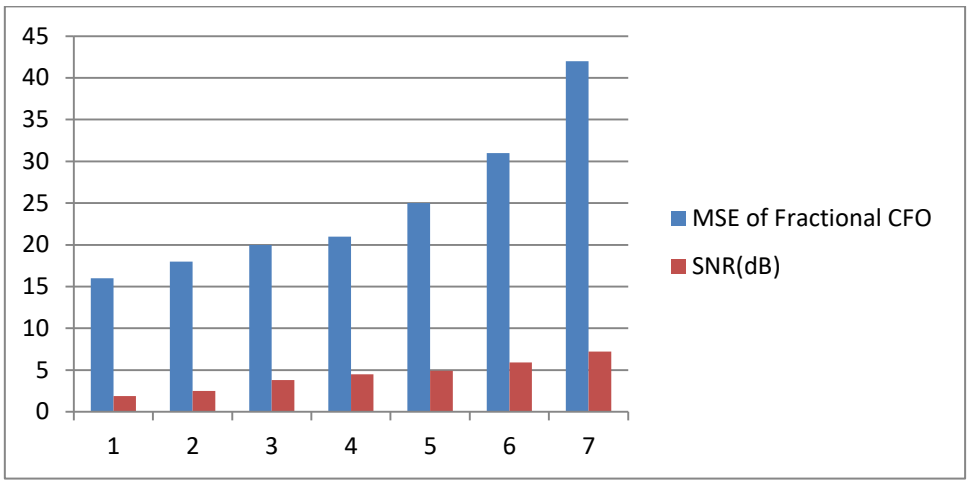

Figure 9: Impact of Imprecise Estimates on CFO Efficiency.

FA	7 bits		6 bits		5 bits		4 bits	
	LUTs	FFs	LUTs	FFs	LUTs	FFs	LUTs	FFs
AC1	81	206	71	198	71	200	61	199
Ac2	81	206	71	198	71	200	61	199
ENE	53	110	42	109	39	186	41	109
Sum	215	522	184	505	181	586	163	507

Table 5: Resources Needed For FPGA To Compute Autocorrelation Metric With Various Word Lengths, Q7.

6.3 Implementation Results

To think about the equipment decrease acquired by utilizing the SOA hardware and that by carrying out the proposed hardware, the past outcomes are presently used to construct three elective executions for the proposed L-DAC1 synchronization. These choices incorporate the following, to be specific.

1) Opt1: A customary utilization of the recommended strategy utilized the hardware displayed in [6] without improving word length (i.e., both fa and fx set to 7).

2) Opt2: An example that has been equipment improved and utilizes the hardware displayed in [6] with f a = 5 and f x = 4.

3) Recommendation: A proposed equipment proficient execution of the recommended connection hardware with f a = 5 and f x = 4.

	LUTs	FFs	DSPs	OPWR	DPWR	FRE
Opt1	5102	6894	15	119.36	0.345	12.63
Opt2	3945	7145	15	119.36	0.308	13.06
Prop	3956	4256	15	116.36	0.412	12.81

Table 6: Resources Used By the Three Instances ofthe Proposed Method With Reduced Complexity

7. CONCLUSION

Due to the added benefit of including a similar device for volatile synchronization in the LDACS OFDM receiver, this study recommends using a multiplier-less connection for spectral acquisition in the computerized LDACS front-end. bottom. This is because, in contrast to the usual ED frameworks and approaching random component detection, the proposed method has an energy reduction of 3 for the multiplier-based correlator and a higher efficiency of LDACS RL contours in the air-to-ground channel. (C. Nanda Kishore and V. Umapathi Reddy, 2006) It has been shown to give dominant discriminative detection. , even at low SNR levels. Also, the perceptual window of spectral acquisition can be as small as the naive RL contour development, resulting in faster progression from acquisition to transmission. Our findings show that the recommended correlator-based spectral acquisition provides 100% detection accuracy even at 12 dB SNR without the need for interference estimation and reduces the processing complexity of the onboard implementation. is showing. L-DACS1 is presented as a response consistent with the more experienced L-band framework to enable high-speed information transmission for the next-generation global ATM framework. In this study, we presented and reviewed an instrumental plan for a unique synchronization procedure for L-DAC1.

REFERENCES

1. A. Langowski, “Fast and accurate OFDM time and frequency synchronisation,” in International Symposium on Wireless Communication Systems. IEEE, 2007, pp. 86–90
2. Ambede, A. P. Vinod, and A. S. Madhukumar, “Design of a low complexity channel filter satisfying LDACS1 spectral mask specifications for air-to-ground communication,” in Proceedings of the Integrated Communications Navigation and Surveillance (ICNS) Conference, April 2016, pp. 7E3:1–7.
3. B. Ronak and S. A. Fahmy, “Multi-pumping flexible DSP blocks for resource reduction on Xilinx FPGAs,” IEEE Transactions on Computer Aided Design of Integrated Circuits and Systems, vol. 36, 2017.
4. C. Nanda Kishore and V. Umapathi Reddy, “A frame synchronization and frequency offset estimation algorithm for OFDM system and its analysis,” EURASIP Journal on Wireless Communications and Networking, vol. 2006, pp. 1–16, 2006
5. Fort, J.-W. Weijers, V. Derudder, W. Eberle, and A. Bourdoux, “A performance and complexity comparison of auto-correlation and crosscorrelation for OFDM burst synchronization,” in IEEE International Conference on Acoustics, Speech, and Signal Processing (ICASSP), vol. 2. IEEE, 2003, pp. II–341.
6. G. Eichinger, K. Chowdhury, and M. Leeser, “Crush: Cognitive radio universal software hardware,” in Proceedings of the International Conference on Field Programmable Logic and Applications (FPL), 2012, pp. 26–32.
7. J. Lotze, S. A. Fahmy, J. Noguera, B. Ozgul, L. E. Doyle, and R. Esser, “Development framework for implementing FPGA-based cognitive network nodes,” in Proceedings of the IEEE Global Telecommunications Conference (GLOBECOM), 2009, pp. 1–7.
8. K. Amiri, Y. Sun, P. Murphy, C. Hunter, J. R. Cavallaro, and A. Sabharwal, “WARP, a unified wireless network testbed for education and research,” in Proceedings of the IEEE International Conference on Microelectronic Systems Education, 2007, pp. 53–54.
9. K. Le, P. Maddala, C. Gutterman, K. Soska, A. Dutta, D. Saha, P. Wolniansky, D. Grunwald, and I. Seskar, “Cognitive radio kit framework: experimental platform for dynamic spectrum research,” ACM SIGMOBILE Mobile Computing and Communications Review, vol. 17, no. 1, pp. 30–39, Jan 2013.
10. K.-W. Yip, Y.-C. Wu, and T.-S. Ng, “Design of multiplierlesscorrelators for timing synchronization in IEEE 802.11 a wireless LANs,” IEEE Transactions on Consumer Electronics, vol. 49, no. 1, pp. 107–114, 2003.
11. R. F. A. Tani and D. Marabissi, “A Low-Complexity Cyclostationary Spectrum Sensing for Interference Avoidance in Femtocell LTE-A-Based Networks,” IEEE Transactions on Vehicular Technology, vol. 65, no. 4, pp. 2747–2753, 2016.
12. S. Shreejith, B. Banarjee, K. Vipin, and S. A. Fahmy, “Dynamic Cognitive Radios on the Xilinx Zynq Hybrid FPGA,” in Proceedings of the International Conference on Cognitive Radio Oriented Wireless Networks (CROWNCOM), 2015, pp. 427–437.
13. T. H. Pham, I. V. McLoughlin, and S. A. Fahmy, “Robust and efficient OFDM synchronization for FPGA-based radios,” Circuits, Systems, and Signal Processing, vol. 33, no. 8, pp. 2475–2493, 2014.

14. T. L.-N. M. Derakhshani and M. Nasiri-Kenari, “Efficient Cooperative Cyclostationary Spectrum Sensing in Cognitive Radios at Low SNR Regimes,” IEEE Transactions on Wireless Communications, vol. 10, no. 11, pp. 3754–3764, 2011.
15. V. K. S. Chaudhari and H. V. Poor, “Autocorrelation-Based Decentralized Sequential Detection of OFDM Signals in Cognitive Radios,” IEEE Transactions on Signal Processing, vol. 57, no. 7, pp. 2690–2700, 2009